








Article

Consecutive Extratropical Cyclones Daniel, Elsa and Fabien, and Their Impact on the Hydrological Cycle of Mainland Portugal

Milica Stojanovic ^{1,*}, Ana Gonçalves ^{1,2}, Rogert Sorí ^{1,2}, Marta Vázquez ^{1,2,3}, Alexandre M. Ramos ¹, Raquel Nieto ², Luis Gimeno ² and Margarida L. R. Liberato ^{1,3}

¹ Instituto Dom Luiz, Faculdade de Ciências da Universidade de Lisboa, 1749-016 Campo Grande, Portugal; ana.redondo.goncalves@uvigo.es (A.G.); roget.sori@uvigo.es (R.S.); martavazquez@uvigo.es (M.V.); amramos@fc.ul.pt (A.M.R.); mlr@utad.pt (M.L.R.L.)

² Centro de Investigación Mariña, Environmental Physics Laboratory (EPhysLab), Campus As Lagoas s/n, Universidade de Vigo, 32004 Ourense, Spain; rnieto@uvigo.es (R.N.); l.gimeno@uvigo.es (L.G.)

³ Escola de Ciências e Tecnologia, Universidade de Trás-os-Montes e Alto Douro, UTAD, 5001-801 Vila Real, Portugal

* Correspondence: mstojanovic@fc.ul.pt

Abstract: The extratropical cyclones that originate in the North Atlantic and propagate towards Europe are one of the major natural hazards in mid-latitudes. In December 2019, three consecutive extratropical cyclones named Daniel, Elsa, and Fabien affected Portugal. In this study, the synoptic and upper-level dynamic conditions associated with these systems during their impact in mainland Portugal are evaluated. The persistent intense zonal flow that crossed the entire Atlantic revealed by the integrated vapor transport and the vertically integrated moisture flux favored these hydro-meteorological systems. The patterns of mean sea level pressure, geopotential, potential vorticity, total column water, and convective available potential energy were used to characterize the influence of every system over mainland Portugal. A cluster analysis of monthly precipitation permitted the classification of the country into four main regions named the Northwest, Centre West, Northeast and Centre East, and South region on which the analysis was focused. The three storms affected every region on consecutive days by the middle of December, producing extreme precipitation events and significant effects on the accumulated rainfall and runoff, particularly in the Northwest, Centre West, Northeast and Centre East regions. As consequence, multiple incidences of damage were reported along mainland Portugal. However, an assessment of the Standardized Precipitation Index (SPI) and the Standardized Precipitation–Evapotranspiration Index (SPEI) on time scales of 1, 3, 6, and 12 months revealed a positive impact of rainfall increase on the attenuation of short and long term accumulated drought conditions, particularly in the center and north regions.

Keywords: extratropical cyclones; heavy precipitation; drought attenuation



Citation: Stojanovic, M.; Gonçalves, A.; Sorí, R.; Vázquez, M.; Ramos, A.M.; Nieto, R.; Gimeno, L.; Liberato, M.L.R. Consecutive Extratropical Cyclones Daniel, Elsa and Fabien, and Their Impact on the Hydrological Cycle of Mainland Portugal. *Water* **2021**, *13*, 1476. <https://doi.org/10.3390/w13111476>

Academic Editor: Letizia Lusito

Received: 10 March 2021

Accepted: 22 May 2021

Published: 24 May 2021

Publisher's Note: MDPI stays neutral with regard to jurisdictional claims in published maps and institutional affiliations.



Copyright: © 2021 by the authors. Licensee MDPI, Basel, Switzerland. This article is an open access article distributed under the terms and conditions of the Creative Commons Attribution (CC BY) license (<https://creativecommons.org/licenses/by/4.0/>).

1. Introduction

Extratropical cyclones are one of the most important characteristics of mid-latitude climate of the Northern Hemisphere, as their passage is often associated with extreme weather conditions such as heavy precipitation and intense winds [1–3]. They are among the most severe weather phenomena that affect the western European countries and a common phenomenon during the boreal winter. Their impacts have been usually associated with considerable social and economic losses (e.g., flooding, landslides, extensive property damage, and human fatalities) [4–9]. Thus, the importance of extratropical cyclones in extreme precipitation events and floods has been analyzed in detail for Europe [10]. For example, Donat et al. (2011) [11] found significant increases in both the strength and frequency of winter storms over large parts of Europe. Furthermore, for the Iberian Peninsula, Liberato and Trigo (2014) [12] showed that extreme precipitation events are

usually triggered by poleward water vapor transport from the tropics and subtropics and under certain conditions by extratropical cyclones. At the sub-monthly scale, extratropical cyclones have a significant impact on the hydrological cycle of the Iberian Peninsula [13] and are one of the primary causes of the occurrence of extreme events over the region (e.g., [6,14]). Portugal and the rest of Europe have been prone to the occurrence of an increasing number of storms with different manifestations and development. For example, on 23 December 2009, the windstorm Xola struck mainland Portugal, causing serious damage in a small area north of Lisbon and in the south region, inflicting economic losses of over EUR 100 million [15]. The variability of the impacts of extratropical cyclones in Portugal and Europe have been documented to depend largely on the influence of different modes of climate variability such as the North Atlantic Oscillation (NAO), East Atlantic (EA), and the Scandinavian Pattern (SCAND) [16]. In particular, the NAO modulates the Atlantic storm tracks during the boreal winter time [17]. However, according to [18] there is no strong evidence for an independent role of storm track variability on rainfall over Portugal.

Several studies have investigated the impacts caused by extratropical cyclones. That is the case of the vast damage caused by the 2017–2019 winter storms in the Azores, Portugal, and other European regions [19–21]. When multiple triggers combine, the impacts associated with extratropical cyclones are often amplified [22] due to multiple hazards occurring simultaneously, such as floods and strong winds. Results of [23] also provided a description and many new features of the sting jets within twenty-nine historic windstorms that affected Europe, a phenomenon that represent a serious hazard. Previous climatic conditions or events such as persistent precipitation can produce soil saturation and increase the vulnerability of the system [24]. In many cases, when extreme weather events occur simultaneously or sequentially, they can overwhelm the ability of natural and human systems to cope, in turn creating social or environmental impacts [3]. The accumulated precipitation from several consecutive cyclones may cause rivers to overflow leading to flooding [25,26]. In this study we use the term consecutive extratropical cyclones to denote two or more disasters that occur successively, and whose direct impacts overlap spatially before recovery from a previous event is considered to be finished [26]. This can include a broad range of multi-hazard types, such as compound events [22] and cascading events [27,28].

Despite the fact that cyclones are normally considered a weather hazard, after a long drought, the rainfall associated with these systems constitutes an important source for the re-establishment of freshwater hydric reserves on the continent, and they contribute to the attenuation of drought conditions or even busting a drought, and so becoming a benefit. This has been documented for tropical cyclones affecting the southeast and east of the United States [29–31], but using a deep search, we did not find any studies regarding the role of extratropical cyclones on the attenuation of drought for mainland Portugal.

During the recent winter of 2019–2020, Europe was hit by three consecutive storms named Daniel, Elsa, and Fabien, which led to serious impacts on the economy, environment, and society, particularly on the Iberian Peninsula (Portugal and Spain, [32,33]). According to the Spanish Agency of Meteorology (AEMET) on the report of storms with great impact for the 2019–2020 season [33], the storm Daniel was formed during the afternoon of 15 December from a secondary low that was located to the west and a few hundred kilometers from Portugal [33]. Extreme rainfall and strong winds associated with storm Daniel hit Portugal on 16 December 2019, which led to flash floods and extensive landslides [32,34,35]. Unlike Daniel, Elsa was formed in the North Atlantic Ocean from a low pressure system formed in the Gulf of Mexico that moved northward along the coast of North America until joining an intense zonal flow that crossed the entire North Atlantic [33], which is known as an Atmospheric River (AR) [36]. In this environment, the system became a deep and wide winter storm named Elsa by the Spanish Agency of Meteorology (AEMET), and it was recognized on synoptic maps on 17 December 2019. The effects most directly associated with Elsa (severe flooding and extreme gusts) occurred in Spain and Portugal from 18

to 20 December 2019. At the end of the life cycle, throughout the 21st of December, Elsa dissipated and was absorbed by the larger circulation of Fabien [33]. The storm Fabien was formed within the same very intense and humid zonal flow (an AR) that crossed the entire Northern Atlantic basin and that a few days before had led to the formation of Elsa. Storms Elsa and Fabien overwhelmed Portugal and Spain with a high amount of precipitation, killing nine people as the countries were hit by widespread flooding and damage [33,37,38].

In this study we present a comprehensive assessment of the synoptic and dynamic characteristics associated with storms Daniel, Elsa, and Fabien during their impact in mainland Portugal, and a description of some of the major damage caused. In addition, we aim to assess the cascading impacts of heavy rainfall on the hydrological cycle of mainland Portugal.

2. Datasets and Methods

2.1. Datasets

The European Centre for Medium Range Weather Forecasts (ECMWF) Reanalysis [39] datasets, namely, mean sea level pressure (MSLP), the vertical integral of northward and eastward water vapor flux, Vertically Integrated Moisture Flux divergence (VIMF), geopotential height (HGT) at 500 hPa, Total column water, Convective Available Potential Energy (CAPE), and the Potential Vorticity (PV) at 250 hPa have been used to analyze the synoptic and dynamics conditions associated to Daniel, Elsa, and Fabien storms during their major impact on mainland Portugal. These fields were extracted for December 2019 at a full temporal (six-hourly) scale, with a horizontal spatial resolution of 0.25° . The vertical integral of northward and eastward water vapor flux which represents the total water vapor flux in the zonal and meridional directions, respectively, are computed on model levels using the specific humidity and zonal and meridional winds, and they are used to calculate integrated vapor transport (IVT). Daily runoff data from ERA5 Land were also used. ERA5 Land is a replay of the land component of the ERA5 climate reanalysis with a higher spatial resolution (~ 9 km).

The latest version of the daily gridded observational precipitation dataset over Europe (E-OBS v.23.1e) was also used in this study. E-OBS comes as an ensemble dataset available with a longitudinal and latitudinal resolution of 0.1° [40] and is freely available at https://surfobs.climate.copernicus.eu/dataaccess/access_eobs.php (Accessed on 24 May 2021). Due to their high resolution, these datasets have been widely utilized to investigate extreme hydro-meteorological events in Europe [41,42]. However, it has been proved that EOBs tend to underestimate the extremes and soften the spatial pattern of precipitation in Europe [43] and particularly in Portugal due to the sparse observational network [44]. For this reason, the ERA5 hourly data of precipitation [45] was used to compute daily mean precipitation values and compare them against E-OBS records. The total precipitation of ERA5 is the sum of large-scale precipitation and convective precipitation. The 95 percentile criterion of daily precipitation of December from 1980 to 2019 was utilized as a threshold to show those days with extreme precipitation in December 2019.

Monthly precipitation, maximum, and minimum temperature obtained from daily values of the E-OBS v.21e dataset from 1980 to 2019 were used to calculate the Standardized Precipitation Index (SPI) [46] and the Standardized Precipitation–Evapotranspiration Index (SPEI) [47] at temporal scales of 1 (SPI1, SPEI1), 3 (SPI3, SPEI3), 6 (SPI6, SPEI6), and 12 (SPI12, SPEI12) months. These datasets were chosen because they provide both precipitation and temperature observational data necessary for the computation of the SPI and SPEI, thus minimizing errors that could arise due to the mixing of different datasets. The SPI and SPEI indices were used to assess the impact of precipitation associated with the storms Daniel, Elsa, and Fabien in December 2019 on short and long term accumulated dry/wet conditions.

2.2. The Ward's Method

The Ward's minimum variance (Ward's method) [48,49] was used to identify homogeneous precipitation zones within Portugal. Ward's method is the most commonly used hierarchical clustering method in climate research which differs from other methods due to the application of the variance analysis approach to estimate the distance between the clusters [50–52]. This method computes the mean values of all variables within each cluster, then computes the Euclidean distance to the cluster mean of each case, and at the end sums all cases. The criterion for selecting which pair of groups will combine in each step is minimizing the sum of squared distances between the points and the centroids of their groups. The Euclidean distance coefficient determines the distance between units where greater distance indicates making different managerial decisions. The result of this method is a tree diagram, showing each phase of hierarchical clustering. Usually, the best number of clusters is not obvious and according to Wilks 2011 [49] establishing the number of groups necessitates a subjective choice that depends on the objectives of the analysis. Ferreira and Hitchcock 2009 [53] compared the performance of different hierarchical clustering techniques such as single linkage, complete linkage, average linkage, and Ward's method. According to their study, the Ward's method did better overall than other hierarchical methods.

2.3. Standardized Precipitation Index (SPI) and Standardized Precipitation Evapotranspiration Index (SPEI)

The SPI [46] and the SPEI [47] were utilized to assess the impact of precipitation associated with the storms Daniel, Elsa, and Fabien in December 2019 on short and long term accumulated dry/wet conditions. Both indices are widely used to monitor and follow dry/wet conditions and are used in a great number of studies [54–63]. The principal difference between these two indices is that the SPI is based on precipitation while SPEI considers the effects of temperature through the atmospheric evaporative demand in the climatic water balance. Therefore, the SPEI combines the changes in the atmospheric evaporative demand with the multiscalar nature of the SPI [64]. The SPI measures anomalies of precipitation comparing observed total precipitation amounts for an accumulation period of interest (1, 3, 6, or 12 months), with the long-term precipitation record for that period. This precipitation record is fitted to a Gamma probability distribution, to transform the original values to standardized units that are comparable in space and time and at different SPI time scales [63,65].

Time series of SPEI for 1980–2019 are calculated using monthly precipitation (PRE) and evapotranspiration (ETo) values averaged over every subregion of Portugal according to the cluster analysis, with the purpose to identify the domain-scale wet and dry climate periods occurrence. The SPEI follows the same conceptual approach of SPI, but it is based on a monthly climatic water balance represented through the Equation (1):

$$D = (PRE - ETo) \quad (1)$$

where D is the water balance over a given period of time, PRE is the precipitation that represents water availability, and ETo represents the atmospheric water demand. The resultant D values in Equation (1) were aggregated at different timescales, following the same procedure as the SPI.

The ETo was calculated using the Hargreaves method [66]. Beguería et al. 2014 [64] described that, compared with the Thornthwaite equation, the SPEI estimated by the Hargreaves equation is very close to that of the Penman–Monteith equation. This method computes ETo as a function of minimum and maximum temperature and extraterrestrial radiation. For calculation of ETo was used the following Equation (2):

$$ETo = 0.0023 \cdot Ra \cdot \left(\sqrt{T_x - T_n} \right) \cdot (T_m + 17.8) \quad (2)$$

where 0.0023 is a constant value; R_a is the extra-terrestrial radiation (derived from the latitude and the month of the year); and T_x , T_n , and T_m are the maximum, minimum, and mean temperature, respectively. Detailed information for calculating SPEI can be found extensively described in [47] and [64]. For the calculation of the SPI and SPEI, the R package is used (<http://cran.r-project.org/web/packages/SPEI>) (Accessed on 24 May 2021). It includes all the recommendations proposed by Beguería et al. [64].

3. Results

3.1. Regionalization of Mainland Portugal Precipitation

Many studies have shown that the distribution of mean annual precipitation in Portugal represents a contrast between north and south as well as between coastal and inland regions [67–69]. The precipitation regionalization made through Ward's method reveals four different regions that are shown in Figure 1a, while the graphical representation of the different districts of Portugal that belong to each region is shown in Figure 1b. The results show that Viana do Castelo, Porto, and Braga represent districts of Portugal with homogeneous precipitation and are classified here as the region named Northwest (NW) region. Viseu, Aveiro, Coimbra, and Leiria belong to the Centre West (CW) region. Northeast and Centre East (NE-CE) region includes Bragança, Vila Real, Castelo Branco, and Guarda while Setúbal, Portalegre, Évora, Beja, Faro, Santarém, and Lisboa districts of Portugal belong to South region.

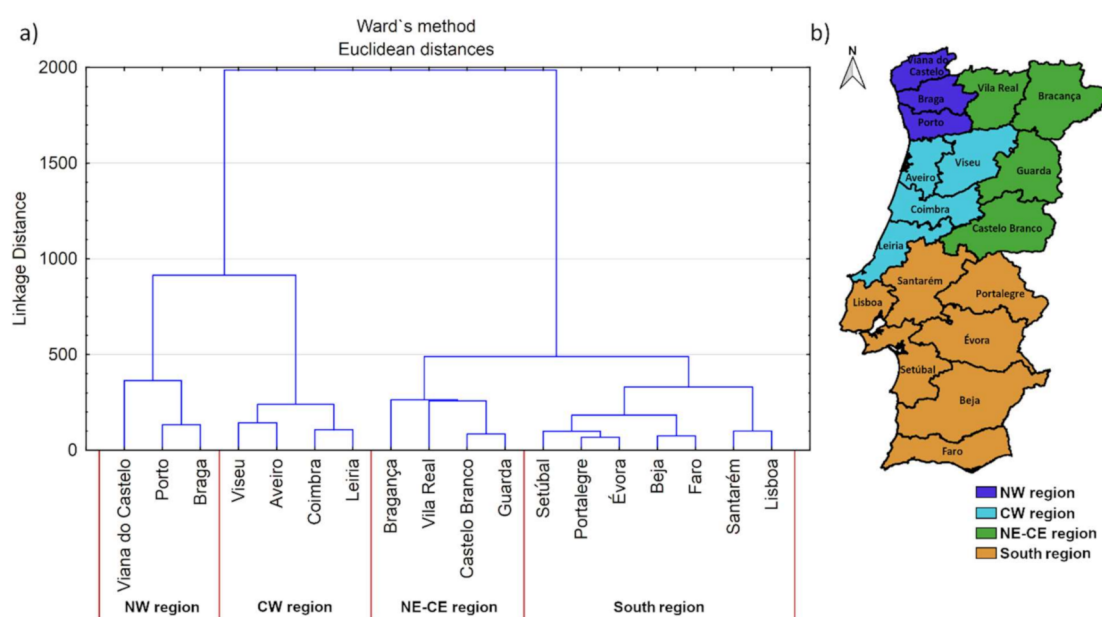


Figure 1. (a) Graphical illustration of Ward's method—the tree diagram with the assigned clusters and (b) schematic representation of the assigned clusters.

3.2. Synoptic Evolution and Upper-Level Dynamic Conditions

Six-hourly maps of the MSLP (shaded) and VIMF (Figure 2a, Figure 3a, and Figure 4a) in addition to the map of the integrated water vapor transport (IVT) that allows us to identify the water vapor/moisture associated with these 3 storms (Figure 2b, Figure 3b, and Figure 4b), the geopotential height (HGT) at 500 hPa and potential vorticity (PV) at 250 hPa (Figure 2c, Figure 3c, and Figure 4c) and the CAPE (Figure 2d, Figure 3d, and Figure 4d) for December 16, 19, and 21 are analyzed.

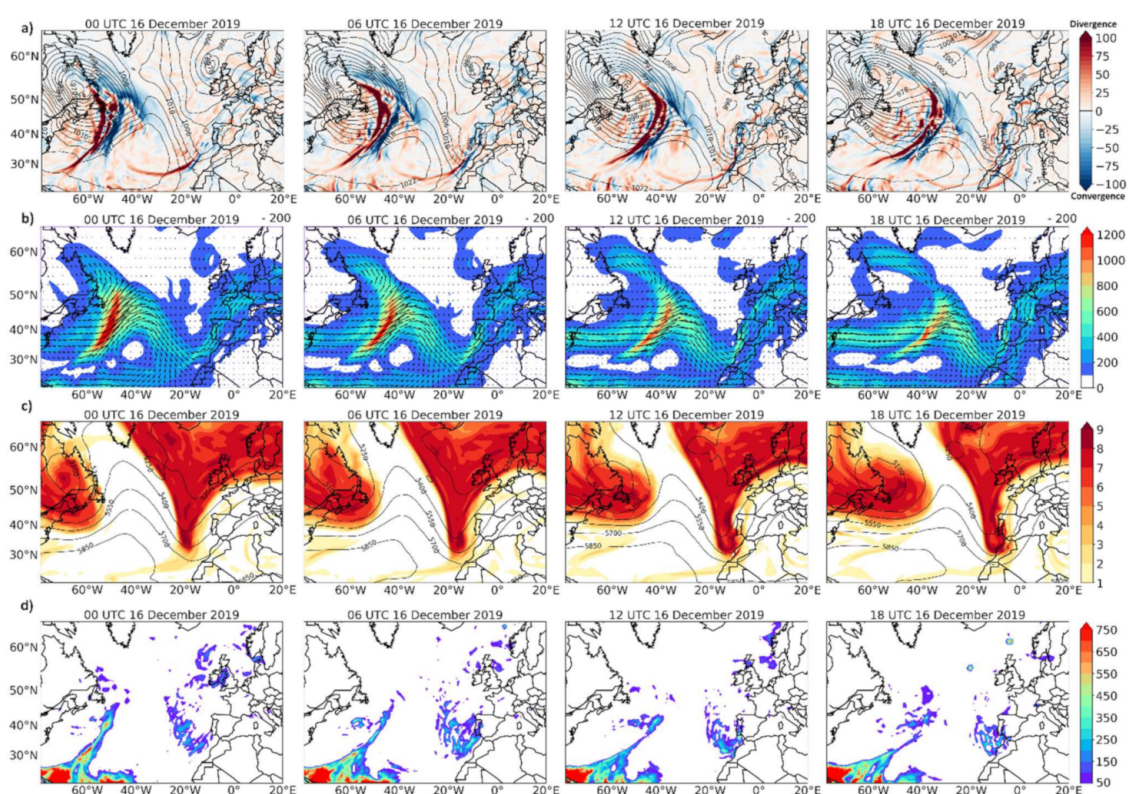


Figure 2. Analysis of the Daniel storm for 16 December 2019 (every six hours: 00, 06, 12, and 18 UTC). (a) VIMF (shaded, mm/day) and MSLP (contour, hPa). (b) IVT (kg/m*s, shaded) intensity and direction (vectors). (c) Potential vorticity at 250 hPa (shaded, PVU) and geopotential height at 500 hPa (contour, gpm). (d) Convective Available Potential Energy (CAPE) (shaded, J/kg).

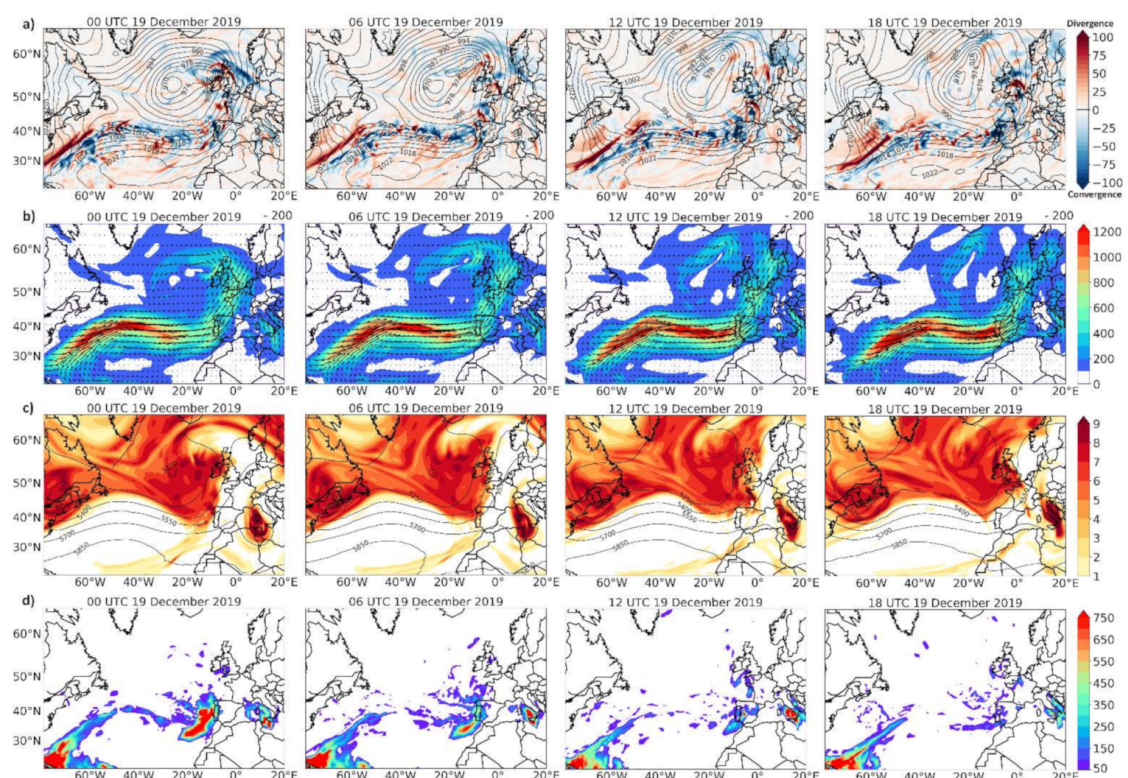


Figure 3. As Figure 2 but for the storm Elsa on 19 December 2019.

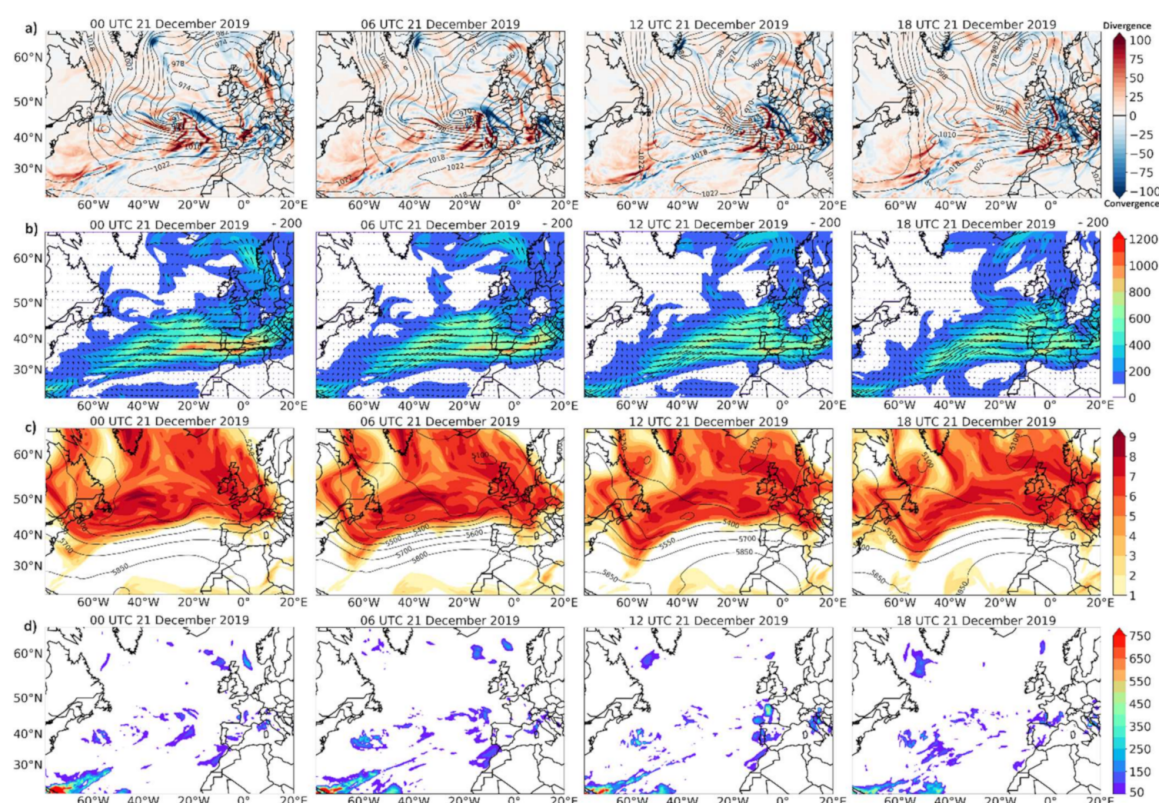


Figure 4. As Figure 2; Figure 3 but for the storm Fabien on 21 December 2019.

The configuration of the MSLP and the geopotential at 500 hPa patterns on December 16 at 00 UTC (Figure 2a,c) reveals a deep trough observed from the surface to upper levels to the west and near of mainland Portugal, which is also visible at higher levels by the intense PV that is mainly observed to the southwest of mainland Portugal (Figure 2c). This trough is the fingerprint of a cold front associated to a low pressure system. At 06:00 UTC a closed isobar is already visible to the southwest of Portugal. To the east of this region and over all of mainland Portugal prevail the vertical upward motions and moisture convergence. The VIMF and IVT (Figure 2a,b) reveal that moisture contribution from the tropical Atlantic favored the formation of Daniel and its development during the following hours, when travelled over the Iberian Peninsula. Previous studies have confirmed that atmospheric water vapor transport revealed by the IVT plays a crucial role on the storms' development [70]. Moreover, the unstable atmospheric conditions diagnosed by CAPE (Figure 2d), show favorable conditions to the development of clouds of vertical development (e.g., cumulonimbus) and consequently for convective precipitation.

For Elsa, the analysis was done for 19 December 2019. On this day, the mainland Portugal received the maximum precipitation of the month (Figure 3). As appreciated in the field of MSLP (Figure 3a), the system moved to the east across the North Atlantic Ocean impacting western Europe. In the four hours, the IVT reveals the fingerprint of a narrow belt of moisture flux from the east coast of North America crossing the Atlantic almost parallel to the isohypse on the HGT 500 hPa map, to finally feed the cyclone. According to AEMET [33] there was a connection between the intensification of Elsa and the moisture flux associated with an Atmospheric River (AR) that crossed the Atlantic, transporting strong water vapor quantity, which may be associated with the IVT narrow belt already described (Figure 2a). The highest values of IVT are centered in the Atlantic Ocean, where mean IVT values range from 800 to 1200 kg/m·s. The four IVT patterns during the influence of Elsa on 19 December differ greatly in the magnitude of moisture transport from the North Atlantic with regard to the climatological pattern of the month (Figure S1. However,

the IVT reaching the mainland Portugal from the east is common both for this day and in the climatological pattern.

At 00 UTC a trough is observed in the geopotential and PV fields (Figure 3c) to the west of mainland Portugal, over the Atlantic Ocean. In the following hours, the strong moisture convergence and high CAPE values over mainland Portugal (Figure 3) in addition to high water content in the atmosphere (Figure S2) are the perfect combination to the occurrence of heavy precipitation.

In Figure 4a the field of MSLP reveals the position and temporal displacement of Fabien during 21 December 2019. At 00 UTC a closed isobar of 974 hPa reveals the center of Fabien at approximately 47° N to the northwest of the Iberian Peninsula over the North Atlantic Ocean. In the following hours, the system moves eastwards affecting mainly the north of the Iberian Peninsula with intense rains, strong winds (>140 km/h), and waves of more than 9 m [71]. As can be seen in the figures, the moisture convergence at the cold front is observed further from the cyclone center and occur over almost all mainland Portugal at 00 and 06 UTC.

In the Iberian Peninsula region, the IVT mean values reach between 600 and 800 kg/m·s. The pattern of IVT, VIMF and total column water (Figure S2) reveal that moisture content downstream from the tropical Atlantic Ocean enhanced Fabien development. The moisture flux convergence along the cold front favored great water content in the atmosphere (Figure S2c) and convective clouds (according to the CAPE values) that prevailed over southern mainland Portugal on 21 December at 00 and 06 UTC, almost over all mainland Portugal on 21 December at 12 UTC, and at 18 UTC over the northern. The result of the combination of these atmospheric and dynamic conditions is to favor the occurrence of heavy precipitation.

3.3. Precipitation Assessment

The daily mean precipitation from October 2019 to January 2020 and the climatological daily precipitation for each of the 4 regions of Portugal is shown in Figure 5a–d. To do it, for each region of study the sum of the total daily precipitation of each grid point was calculated and divided by the total number of these grids, respectively. Thus, a precipitation value is obtained that characterizes the entire study area of each region. High precipitation over the four regions of study on day 16 of December was associated with the storm Daniel. The greater rainfall occurred in the NW, followed by the CW, NE-CE, and the south region. However, these values could be underestimated, as already described in Section 2.1. Indeed, the precipitation from ERA5 for this day (Figure S3) was greater than that obtained from E-OBS for each subregion. In the following days, the contribution of Elsa and Fabien is observed. The accumulated rainfall on December 19 stands out due to the influence of Elsa, with extreme values above the 95th percentile in all regions. On this day, the major rainfall occurred in the NW region, followed by the CW, NE-CE, and south region. The ERA5 also reflects greater values than those obtained with E-OBS after 19 December, but daily precipitation values for December of 1980 to 2019 from both datasets show a positive, high (>0.92), and statistically significant correlation in each region (Figure S3). These results are in correspondence with those published by the Instituto Português do Mar e da Atmosfera (IPMA) in its climatological report for December 2019 [32].

From December 15 occurred a cascading impact of precipitation that is observed in the daily accumulated precipitation (Figure 5e). The precipitation over each region associated with these systems from December 16 to 22 accounted for 58.27%, 75%, 70.98%, and 88.22 of the mean precipitation of the month and 22.39%, 28.25%, 31.79%, and 28.66% for each cluster of the mean precipitation accumulated from October to December 2019 (Table 1).

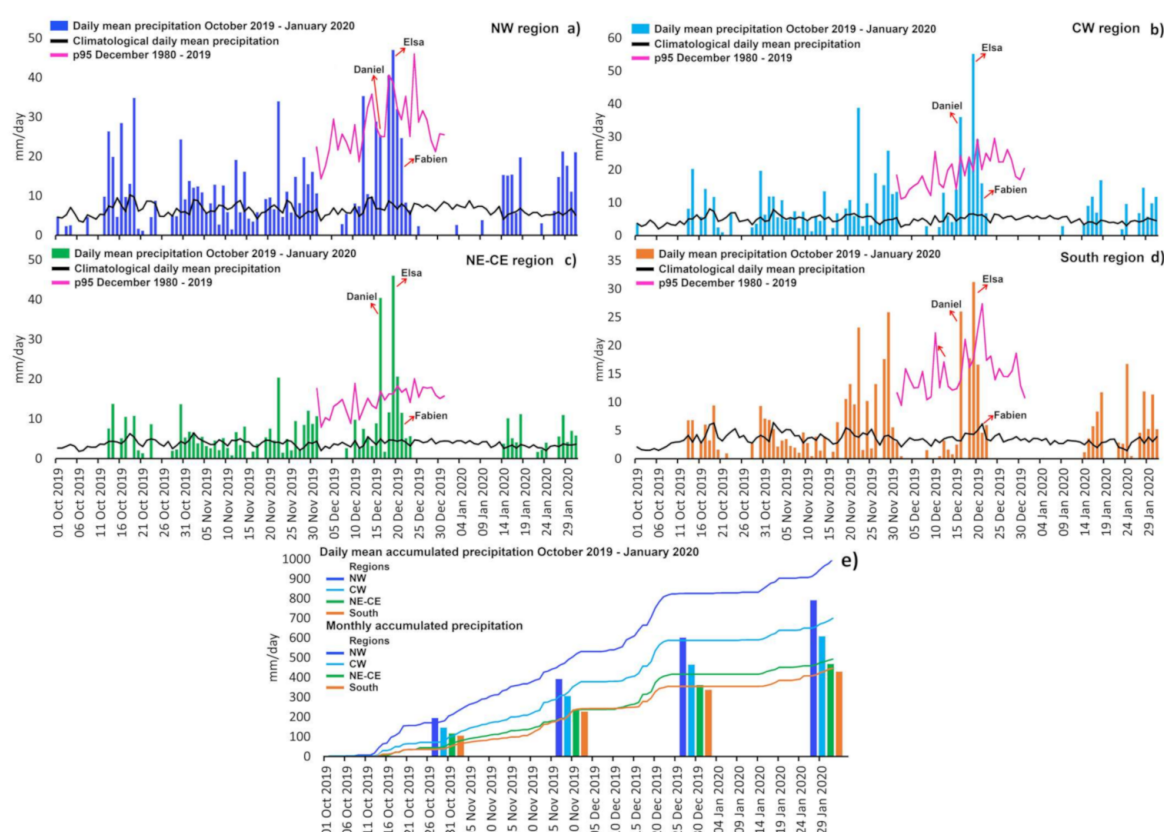


Figure 5. Daily mean precipitation from October to December 2019 (bars) and climatological daily mean precipitation over 4 regions of Portugal for 1980–2019 (lines) (a–d) and the daily mean accumulated precipitation from October to December 2019 and the monthly accumulated climatological precipitation for 1980–2019 (e).

Table 1. Percentage of the precipitation from 16 to 22 December with regards to mean precipitation accumulated for December 2019, and from October to December 2019.

Accumulated Precipitation (%)	NW Region	CW Region	NE-CE Region	South Region
December 2019	58.27	75	70.98	88.22
October to December 2019	22.39	28.25	31.79	28.66

The spatial pattern of anomalies of precipitation calculated using E-OBS dataset, ERA5 dataset and runoff from ERA5 Land datasets in Portugal from 16 to 22 December appears in Figure 6. Despite the fact that on December 15th the average accumulated precipitation is significant over mainland Portugal, according to the Spanish Agency of Meteorology (AEMET), the storm Daniel affected the Iberian Peninsula on December 16th. On this day, positive anomalies of the precipitation occurred in all mainland Portugal, but most intensely in the north. On 17 December, a decrease of the accumulated precipitation brought negative anomalies at spatial scale in all Portugal mainland (Figure 6a). However, the memory of intense rainfall in previous two days made possible the occurrence of positive runoff anomalies, in the northwest and center west regions (Figure 6c). The major precipitation occurred on 19 December. This day the most intense positive anomalies of the precipitation and runoff occurred over the center and half north of Portugal. Similar but less intense patterns of precipitation and runoff are observed until 22 December. This is in agreement with [72], who found that frequencies of occurrence of cyclonic atmospheric circulation regimes are largely dominant in the interannual variability of the winter rainfall throughout mainland Portugal, but principally over the north.

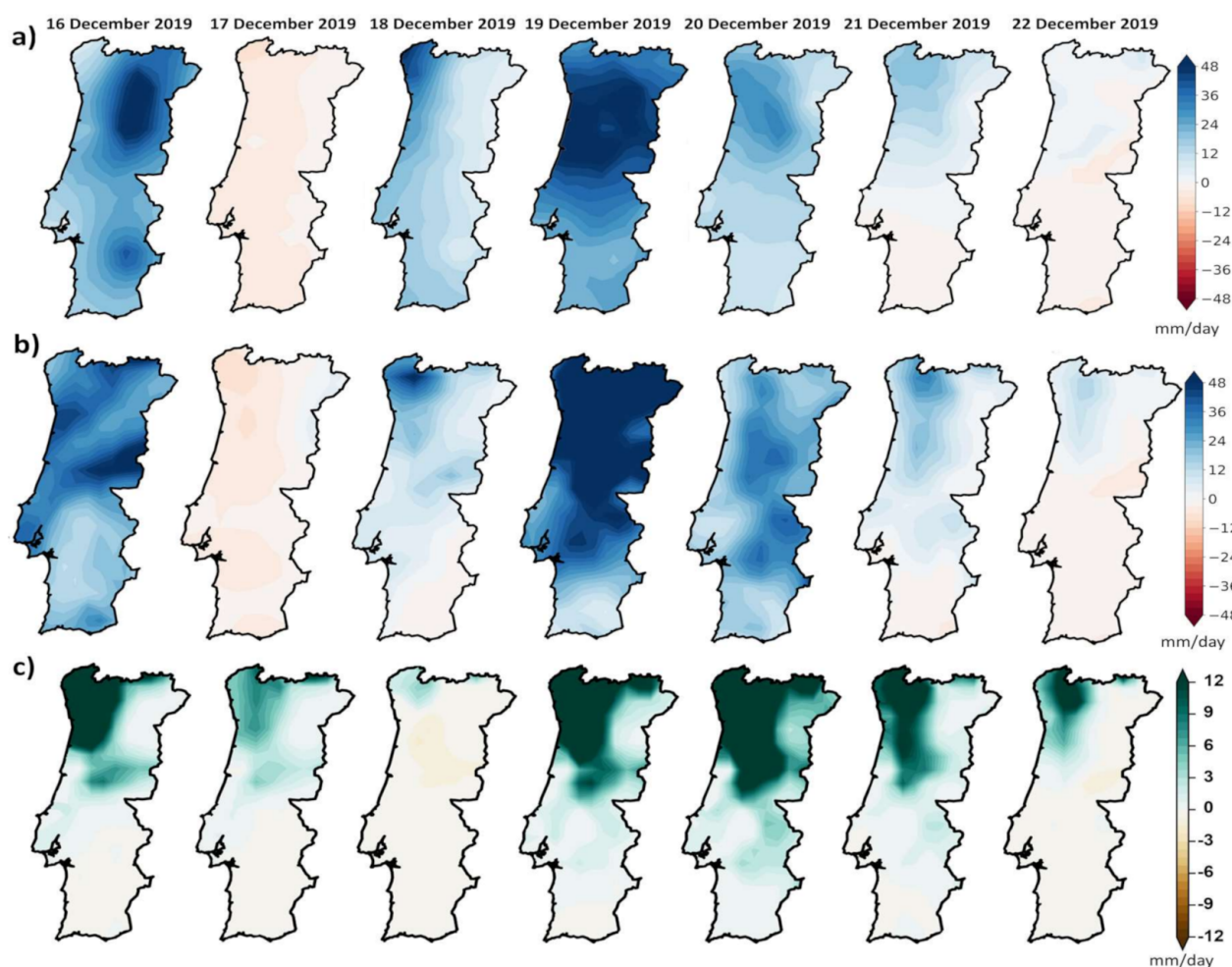


Figure 6. Precipitation anomaly (mm/day) calculated using EOBS data (a) ERA5 data (b) and runoff anomaly (mm/day) (c) during Daniel, Elsa, and Fabien storms from 16 to 22 December 2019.

Because E-OBS precipitation has been characterized by underestimation, the spatial anomaly of daily precipitation was also calculated using ERA5 data. The results shown in Figure 6b show that there are some differences in the spatial pattern of the anomalies. For December 16, ERA5 also shows the highest values of anomalies in the central and northern regions. However, the maximum values are located towards the coast and extreme north of the country, while the E-OBS precipitation anomalies show the maximum value towards the center of northern mainland Portugal. On the 17th, the anomalies of both data sets coincide in the prevalence of positive anomalies throughout the territory. On the 18th, the anomalies obtained by E-OBS exceed those obtained with ERA5 data, while on the 19th, under the influence of Elsa, both patterns coincide in the occurrence of the largest anomalies, mainly in the northern region of Portugal, although ERA5 shows higher values. In the following days (20–22 December), it is also observed that the pattern of anomalies obtained with ERA5 is greater, especially on 20 December over the central region of Portugal.

3.4. Impacts on the Hydrological Cycle

The primary impact of intense rainfall on the evolution of dry/wet conditions in every region of study due to the cascading influence of the extratropical cyclones Daniel, Elsa, and Fabien were assessed. Figure 7 shows the temporal evolution of the SPI (left panel) and the SPEI (right panel) at 1, 3, 6, and 12-months' time scale for each study region of Portugal in the period March 2019–February 2020. As observed, the SPI1 computed for every region shows great variability, but also a great similarity among the regions. In

December 2019, wet conditions are identified for every region, which were also observed in the previous month. In both months, the major differences in the magnitude of the SPI are appreciated between the northern regions and the south region. This difference increases when comparing the magnitude of the SPI in the rest of the time scales, and more clearly between the NW, CW, and the south region. The SPI3 reveals better the importance of accumulated precipitation in November and December for the recovery of dry conditions identified in September and October, whereas the SPI6 is better for those observed in October. Highlighting October 2019, dry conditions, according to the SPI 3 and SPI6, affected simultaneously all four regions, intensifying drought severity from the north to the south of the country. The precipitation of November and December favored the recovery of drought, with the highest positive values of the SPI3 and SPI6 in December indicating moderate wet conditions in the NW, NE-CE, and CW regions. However, in the south region are only identified wet conditions through the SPI1, while the SPI3 and SPI6 just reveal near normal conditions. After December 2019, the SPI1, SPI3, and SPI6 all decrease. At a longer temporal scale (12 months), the SPI remained negative previous to December, indicating the prevalence of dry conditions. The effect of intense accumulated precipitation during December permitted busting drought conditions accumulated from March 2019 (9 months) in the NW, NE-CE, and CW regions. However, the SPI12 of December 2019 for the south region revealed that despite becoming less dry than November, the SPI still remains negative.

The SPI3 reflects short-term and medium-term moisture conditions and provides a seasonal estimation of precipitation. It is primarily utilized for assessing agricultural drought [65]. In addition, the SPI6 can be very effective in showing the precipitation over distinct seasons and give information associated with anomalous streamflow and reservoir levels, depending on the region and time of year [65]. This application of the index may be utilized to disentangle the influence of precipitation associated with extratropical cyclones on water volumes, river flows, reservoirs, and its importance for agriculture and generation of electricity in Portugal.

The same analysis through the SPEI (Figure 7 right panel) reveals similar findings as described with the SPI. However, the attenuation of accumulated drought conditions revealed by the temporal evolution of the SPEI6 and SPEI12 is less abrupt than that observed with the SPI6 and SPI12. The effect of evapotranspiration is noticeable in the magnitude of drought conditions accumulated through the SPEI12. This is clearly observed in December, when, despite large accumulations of precipitation especially in central and northern Portugal, the SPEI does not reach positive values. After December 2019 and until February 2020, the values of SPEI1, SPEI3, and SPEI6 decrease, as does SPEI12 for the south region, but they increase in the other study regions in Portugal.

3.5. Socioeconomic Impacts of Daniel, Elsa, and Fabien

All three studied storms had strong winds with wind gusts of up to 150 km/h [32] that caused numerous adverse impacts and several people were injured. Associated with strong winds, these storms had large amounts of moisture and water vapor, which gave rise to events of heavy precipitation, thus causing sudden floods in many places, and therefore vast damage [32,33]. With the passage of the first storm, Daniel, the Portuguese civil protection services registered 200 incidents, mainly floods [35]. Starting from December 19, Elsa, the most severe storm out of these three storms, affected Portugal. This storm severely affected Portugal, where it caused more than 6237 occurrences, including many fallen trees, 2 fatalities, and 70 people were forced to be evacuated from their homes according to the National Emergency and Civil Protection Authority [73].

In the Coimbra District (Mondego River Basin) which belongs to the CW region, the strong winds and heavy precipitation flooded rivers, brought down power lines, uprooted trees, and disrupted rail across the regions. It was necessary to evacuate the local population as a precaution due to the rising waters and risk of flooding. [74]. Figure 8 shows the flood event delineation in the area of Coimbra after floods and a dike breach.

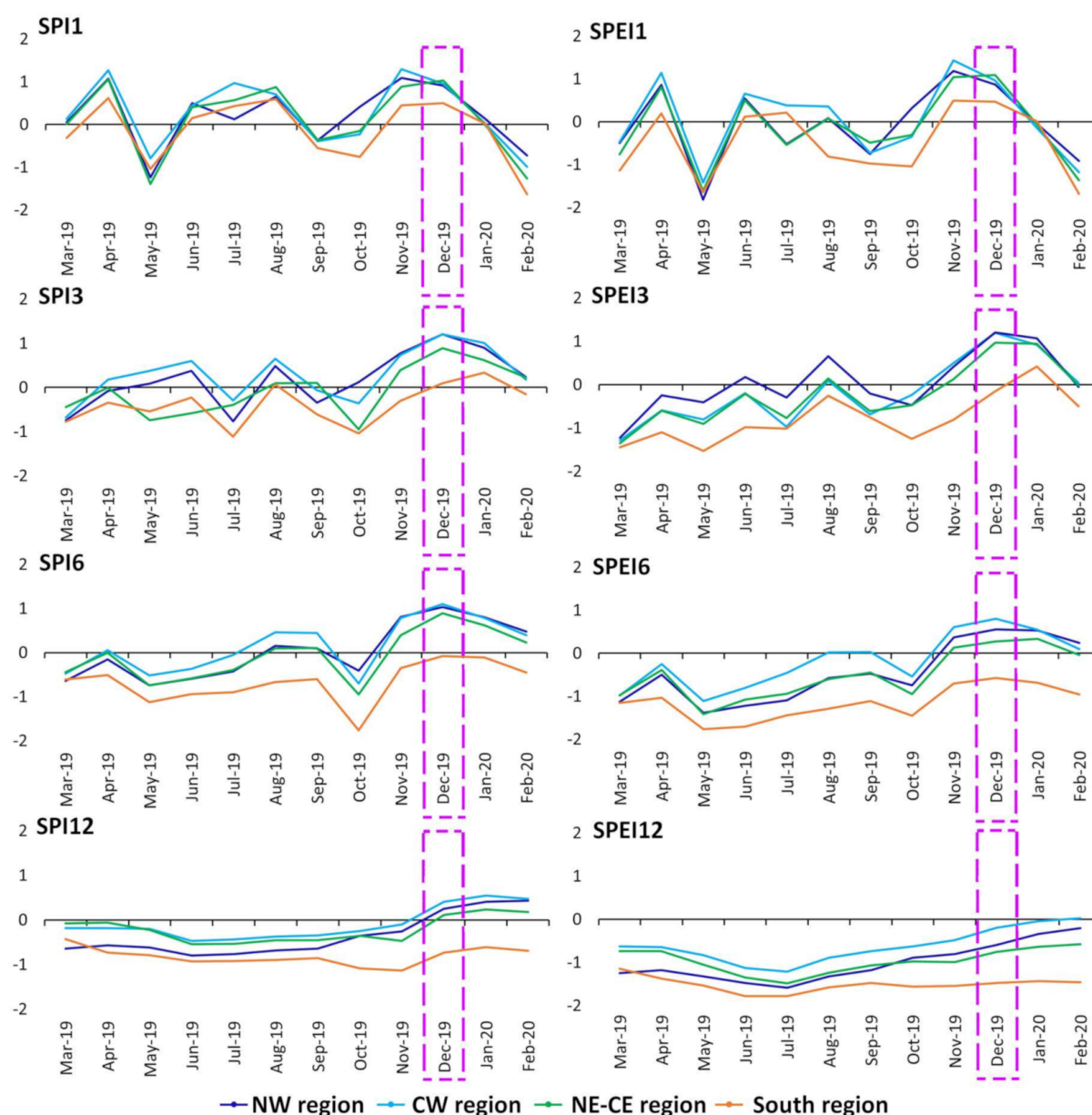


Figure 7. Temporal evolution of the SPI (left) and the SPEI (right) at temporal scales of 1, 3, 6, and 12 months for mainland Portugal for the period: March 2019–February 2020. Box of discontinued magenta lines indicates the month of impact (December) by Daniel, Elsa, and Fabian in mainland Portugal.

The storm Elsa, between December 19 and 20, which was joined on December 21 by the Fabien depression, caused damage to homes (roofs blown off), train lines, roads, and the power lines, affecting the distribution of energy of thousands of people, especially in the north and center of the country. The electricity distribution infrastructures were significantly affected, nearly 2 million people registered that lost access to electricity as a direct consequence of the event. These incidents were largely caused by high gusts of wind in the north and center of the country which uprooted numerous trees, blew down electricity masts, and blew roofs away. In the region of Fajão (Coimbra District) there were reported gusts of 150 km/h, in São Pedro do Sul (Viseu District) of 145 km/h, and at the Guarda District, 136 km/h. In addition to these values, the records of anemometers installed in several wind farms were similar and also high, with 178 km/h in Arganil (Coimbra District), 177 km/h in Vila Pouca de Aguiar (Vila Real District), and 173 km/h in Ourém (Santarém District) [32,75].

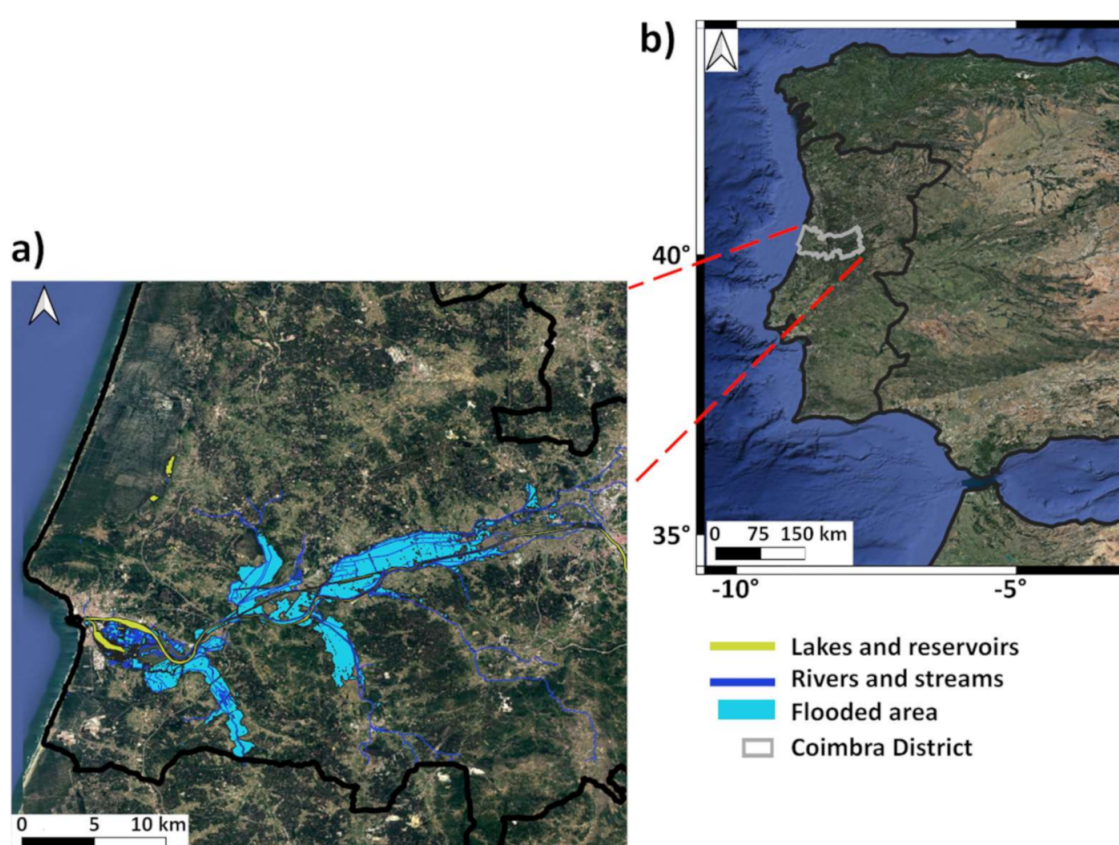


Figure 8. Floods area and dike breaches occurred in Coimbra—Mondego River Basin. The map (a) shows the flood event delineation in the area of Coimbra District (Portugal) on 23 December 2019. The location of Coimbra District in Portugal (b). Vector data obtained from [76].

Up until December 22 of 2019, the strong effects of severe weather had caused two fatalities, one missing person, 144 people displaced, and 352 people displaced by precaution, with over 11 600 occurrences in mainland Portugal, mostly floods and fallen trees. Moreover, according to information from the Portuguese Insurance Association, the damage caused by the storms Elsa and Fabien is around 34 million euros, in which almost 17,000 claims were covered by insurance policies [37].

These numbers allow us to see the severity of these meteorological phenomena. Firstly, in Portugal and Spain, and then along with Europe, the impacts were many and the main problem is that people are not prepared for these situations. Although the forecasts of the meteorological systems are more and more accurate, it is not yet possible to predict with total certainty its trajectory and the intensity of meteorological impacts. Thus, it is extremely important to share information between meteorological services, the responsible civil authorities, and populations, so that they can minimize the serious impacts associated with these extreme events.

4. Conclusions

Three consecutive extratropical cyclones, named Daniel, Elsa, and Fabien affected mainland Portugal during December 2019. The moisture contribution from the tropical Atlantic was associated with the development before, and during, the impact of each system. The patterns of the IVT revealed an atmospheric river associated with the Elsa and Fabien development. From 15 December to 21 December the three systems were associated with moisture convergence, high water content, and unstable atmospheric conditions over mainland Portugal. It led to extreme precipitation events and consequently strong positive anomalies of precipitation and runoff, which were mainly observed in the NW, NE-CE, and CW regions. These regions were determined after a regionalization process applying a

clustering method and using monthly values of precipitation for 18 districts occupying the whole of mainland Portugal. The rainfall contribution of these systems represented more than 58% of the mean precipitation of December 2019 in the NW, CW, and NE-CE regions, but more than 88% in the South region.

The associated impacts of these systems were reported as negative. According to official reports, the effect of heavy rainfall, strong winds, and waves associated with these systems produced serious damage to the Portuguese economy, and other irreparable damage due to the loss of human lives.

According to the temporal evolution of the SPI and the SPEI at temporal scales of 1, 3, 6, and 12 months, the contribution of heavy rainfall associated with Daniel, Elsa, and Fabien significantly increased the precipitation of December 2019 in respect of the climatological values. This favored the attenuation and busting of drought conditions accumulated from previous months in all the study regions, but particularly in the south. This is also seen more clearly in the 6- and 12-month time scale of both the SPI and SPEI. In the following two months after the impact of Daniel, Elsa, and Fabien, both the SPI and the SPEI values at temporal scales of 1, 3, and 6 months decreased. Nevertheless, it is less noticeable in the SPI12, and does not happen with the SPEI12 for the northwest, northeast, and center regions. This confirms that extratropical cyclones also play a crucial role on the country's mainland hydrological cycle. Deep research is ongoing to address the impact of the winter storm's precipitation on the water balance at interannual time scales, the attenuation of drought conditions, river levels, the amount of available fresh water storage, and the possible impacts or benefit in agriculture and the hydro energy sector.

Supplementary Materials: The following are available online at <https://www.mdpi.com/article/10.3390/w13111476/s1>. Figure S1: The average pattern of the IVT for December (period 1980–2019). Figure S2: The pattern of total column water (units: kg/m²) for (a) the Daniel storm for 16 December 2019, (b) Elsa storm for 19 December 2019, and (c) Fabien storm for 21 December 2019 (every six hours: 00, 06, 12, and 18 UTC). Figure S3: Daily precipitation from E-OBS (blue bars) and ERA5 (orange bars) for December 2019. R values represent the correlation between both series.

Author Contributions: M.S., A.G., R.S. and M.V., conceived the idea of the study, processed the data, analyzed the results, and revised the manuscript. A.M.R., R.N., L.G. and M.L.R.L. analyzed the results and revised the manuscript. All authors have read and agreed to the published version of the manuscript.

Funding: Fundação para a Ciência e a Tecnologia (UIDB/50019/2020–IDL); Fundação para a Ciência e a Tecnologia and Portugal Horizon2020 project “Weather Extremes in the Euro Atlantic Region: Assessment and Impacts–WEx–Atlantic” (PTDC/CTAMET/29233/2017). Xunta de Galicia: Project ED431C 2017/64–GRC; Ministerio de Ciencia, Innovación y Universidades: RTI2018-095772-B-I00.

Institutional Review Board Statement: Not applicable.

Informed Consent Statement: Not applicable.

Data Availability Statement: Not applicable.

Acknowledgments: We acknowledge the E-OBS dataset from the EU-FP6 project UERRA (<https://www.uerra.eu>) and the Copernicus Climate Change Service, and the data providers in the ECA&D project (<https://www.ecad.eu>) (Accessed on 24 May 2021). R.S. and M.V. acknowledge the postdoctoral fellowship ED481B 2019/070, and ED481B 2018/062 from the Xunta of Galicia. A. M. R. was supported by the Scientific Employment Stimulus 2017 from FCT (CEECIND/00027/2017).

Conflicts of Interest: The authors declare no conflict of interest.

References

1. Ulbrich, U.; Leckebusch, G.C.; Pinto, J.G. Extra-tropical cyclones in the present and future climate: A review. *Theor. Appl. Clim.* **2009**, *96*, 117–131. [[CrossRef](#)]
2. Catto, J.L.; Ackerley, D.; Booth, J.F.; Champion, A.J.; Colle, B.A.; Pfahl, S.; Pinto, J.G.; Quinting, J.F.; Seiler, C. The Future of Midlatitude Cyclones. *Curr. Clim. Chang. Rep.* **2019**, *5*, 407–420. [[CrossRef](#)]

3. Dacre, H.F.; Pinto, J.G. Serial clustering of extratropical cyclones: A review of where, when and why it occurs. *NPJ Clim. Atmos. Sci.* **2020**, *3*, 1–10. [\[CrossRef\]](#)
4. Kovats, R.S.; Valentini, R.; Bouwer, L.M.; Georgopoulou, E.; Georgopoulou, D.; Jacob, E.; Martin, E.; Rounsevell, M.; Soussana, J.F. *Climate Change 2014: Impacts, Adaptation, and Vulnerability. Part B: Regional Aspects. Contribution of Working Group II to the Fifth Assessment Report of the Intergovernmental Panel on Climate Change*; Barros, V.R., Field, C.B., Dokken, D.J., Mastrandrea, M.D., Mach, K.J., Bilir, T.E., Chatterjee, M., Ebi, K.L., Estrada, Y.O., Genova, R.C., et al., Eds.; Cambridge University Press: Cambridge, UK; New York, NY, USA, 2014; pp. 1267–1326.
5. Munich Re: Natural Catastrophes 2014, Analyses, Assessments, Positions, TOPICS-GEO 2013, Munich, 67. Available online: https://www.munichre.com/content/dam/munichre/contentlounge/website-pieces/documents/302-08121_en.pdf/_jcr_content/renditions/original/302-08121_en.pdf (accessed on 24 May 2021).
6. Liberato, M.L.R.; Pinto, J.G.; Trigo, R.M.; Ludwig, P.; Ordóñez, P.; Yuen, D.; Trigo, I.F. Explosive development of winter storm Xynthia over the subtropical North Atlantic Ocean. *Nat. Hazards Earth Syst. Sci.* **2013**, *13*, 2239–2251. [\[CrossRef\]](#)
7. Liberato, M.L. The 19 January 2013 windstorm over the North Atlantic: Large-scale dynamics and impacts on Iberia. *Weather Clim. Extremes* **2014**, *5–6*, 16–28. [\[CrossRef\]](#)
8. Fink, A.H.; Pohle, S.; Pinto, J.G.; Knippertz, P. Diagnosing the influence of diabatic processes on the explosive deepening of extratropical cyclones. *Geophys. Res. Lett.* **2012**, *39*, 07803. [\[CrossRef\]](#)
9. Paprotny, D.; Sebastian, A.; Morales-Nápoles, O.; Jonkman, S.N. Trends in flood losses in Europe over the past 150 years. *Nat. Commun.* **2018**, *9*, 1–12. [\[CrossRef\]](#)
10. Hawcroft, M.; Walsh, E.; Hodges, K.; Zappa, G.; Hawcroft, M. Significantly increased extreme precipitation expected in Europe and North America from extratropical cyclones. *Environ. Res. Lett.* **2018**, *13*, 124006. [\[CrossRef\]](#)
11. Donat, M.G.; Renggli, D.; Wild, S.; Alexander, L.V.; Leckebusch, G.C.; Ulbrich, U. Reanalysis suggests long-term upward trends in European storminess since 1871. *Geophys. Res. Lett.* **2011**, *38*, 14703. [\[CrossRef\]](#)
12. Liberato, M.L.R.; Trigo, R.M. Extreme precipitation events and related impacts in western Iberia. Hydrology in a changing world: Environmental and human dimensions. In Proceedings of the 7th FRIEND-Water, Montpellier, France, 7–10 October 2014.
13. Trigo, R.M.; Osborn, T.J.; Corte-Real, J.M. The North Atlantic Oscillation influence on Europe: Climate impacts and associated physical mechanisms. *Clim. Res.* **2002**, *20*, 9–17. [\[CrossRef\]](#)
14. Liberato, M.L.R.; Pinto, J.G.; Trigo, I.; Trigo, R.M. Klaus—An exceptional winter storm over northern Iberia and southern France. *Weather* **2011**, *66*, 330–334. [\[CrossRef\]](#)
15. Pinto, P.; Belo-Pereira, M. Damaging Convective and Non-Convective Winds in Southwestern Iberia during Windstorm Xola. *Atmosphere* **2020**, *11*, 692. [\[CrossRef\]](#)
16. Trigo, R.M.; Valente, M.A.; Trigo, I.; Miranda, P.M.A.; Ramos, A.; Paredes, D.; García-Herrera, R. The Impact of North Atlantic Wind and Cyclone Trends on European Precipitation and Significant Wave Height in the Atlantic. *Ann. N. Y. Acad. Sci.* **2008**, *1146*, 212–234. [\[CrossRef\]](#)
17. Luo, D.; Diao, Y.; Feldstein, S.B. The Variability of the Atlantic Storm Track and the North Atlantic Oscillation: A Link between Intraseasonal and Interannual Variability. *J. Atmos. Sci.* **2011**, *68*, 577–601. [\[CrossRef\]](#)
18. Ulbrich, U.; Christoph, M.; Pinto, J.; Corte-Real, J. Dependence of winter precipitation over Portugal on NAO and baro-clinic wave activity. *Int. J. Climatol.* **1999**, *19*, 379–390. [\[CrossRef\]](#)
19. Vautard, R.; Van Oldenborgh, G.J.; Otto, F.E.L.; Yiou, P.; De Vries, H.; Van Meijgaard, E.; Stepek, A.; Soubeyroux, J.-M.; Philip, S.; Kew, S.F.; et al. Human influence on European winter wind storms such as those of January 2018. *Earth Syst. Dyn.* **2019**, *10*, 271–286. [\[CrossRef\]](#)
20. Lü, Z.; Li, F.; Orsolini, Y.J.; Gao, Y.; He, S. Understanding of European Cold Extremes, Sudden Stratospheric Warming, and Siberian Snow Accumulation in the Winter of 2017/18. *J. Clim.* **2020**, *33*, 527–545. [\[CrossRef\]](#)
21. Gonçalves, A.; Loureiro, S.; Hénin, R.; Liberato, M.L.R. Extreme Storms over the Iberian Peninsula during 2017–2018 Extended Winter: Synoptic Conditions and Impacts. In Proceedings of the II International Conference Risks, Security and Citizenship Proceedings, Sétubal, Portugal, 28–29 March 2019; pp. 22–25.
22. Zscheischler, J.; Westra, S.; Hurk, B.J.J.M.V.D.; Seneviratne, S.I.; Ward, P.J.; Pitman, A.; AghaKouchak, A.; Bresch, D.N.; Leonard, M.; Wahl, T.; et al. Future climate risk from compound events. *Nat. Clim. Chang.* **2018**, *8*, 469–477. [\[CrossRef\]](#)
23. Hewson, T.D.; Neu, U. Cyclones, windstorms and the IMILAST project. *Tellus A Dyn. Meteorol. Oceanogr.* **2015**, *67*. [\[CrossRef\]](#)
24. Zscheischler, J.; Martius, O.; Westra, S.; Bevacqua, E.; Raymond, C.; Horton, R.M.; Hurk, B.V.D.; AghaKouchak, A.; Jézéquel, A.; Mahecha, M.D.; et al. A typology of compound weather and climate events. *Nat. Rev. Earth Environ.* **2020**, *1*, 333–347. [\[CrossRef\]](#)
25. Priestley, M.D.K.; Pinto, J.G.; Dacre, H.F.; Shaffrey, L.C. The role of cyclone clustering during the stormy winter of 2013/2014. *Weather* **2017**, *72*, 187–192. [\[CrossRef\]](#)
26. de Ruiter, M.C.; Couasnon, A.; Homberg, M.J.V.D.; Daniell, J.E.; Gill, J.C.; Ward, P.J. Why We Can No Longer Ignore Consecutive Disasters. *Earths Futur.* **2020**, *8*, e2019EF001425. [\[CrossRef\]](#)
27. Pescaroli, G.; Alexander, D. A definition of cascading disasters and cascading effects: Going beyond the “toppling dominos” metaphor. *Planeta Risk* **2015**, *3*, 58–67.
28. Zuccaro, G.; De Gregorio, D.; Leone, M.F. Theoretical model for cascading effects analyses. *Int. J. Disaster Risk Reduct.* **2018**, *30*, 199–215. [\[CrossRef\]](#)

29. Maxwell, J.T.; Ortengren, J.T.; Knapp, P.A.; Soulé, P.T. Tropical Cyclones and Drought Amelioration in the Gulf and Southeastern Coastal United States. *J. Clim.* **2013**, *26*, 8440–8452. [CrossRef]
30. Maxwell, J.T.; Soulé, P.T.; Ortengren, J.T.; Knapp, P.A. Drought-Busting Tropical Cyclones in the Southeastern Atlantic United States: 1950–2008. *Ann. Assoc. Am. Geogr.* **2012**, *102*, 259–275. [CrossRef]
31. Kam, J.; Sheffield, J.; Yuan, X.; Wood, E.F. The Influence of Atlantic Tropical Cyclones on Drought over the Eastern United States (1980–2007). *J. Clim.* **2013**, *26*, 3067–3086. [CrossRef]
32. Instituto Português do Mar e da Atmosfera—IPMA. 2019. Available online: http://www.ipma.pt/resources.www/docs/im.publicacoes/edicoes.online/20200123/gUybHojZlxtWdawgmvjf/cli_20191201_20191231_pcl_mm_co_pt.pdf (accessed on 8 March 2021).
33. Agencia Estatal Meteorología—AEMET. 2019. Available online: http://www.aemet.es/documentos/es/serviciosclimaticos/vigilancia_clima/resumenes_climat/mensuales/2019/res_mens_clim_2019_12.pdf (accessed on 8 March 2021).
34. Cmjournal. 2019. Available online: <https://www.cmjournal.pt/sociedade/detalhe/tempo--tempestade-daniel-deixa-pais-sob-aviso-amarelo-com-neve-chuva-e-vento-forte> (accessed on 8 March 2021).
35. RTP. 2019. Available online: https://www.rtp.pt/noticias/pais/protecao-civil-registou-200-incidentes-com-a-tempestade-daniel_v1192383 (accessed on 8 March 2021).
36. Egimeno, L.; Enieto, R.; Vázquez, M.; Lavers, D.A. Atmospheric rivers: A mini-review. *Front. Earth Sci.* **2014**, *2*. [CrossRef]
37. SicNoticias. 2019. Available online: <https://sicnoticias.pt/pais/2019-12-22-Depressao-Elsa-e-Fabien-deixam-rasto-de-destruicao-de-norte-a-sul-do-pais>. (accessed on 8 March 2021).
38. Zap.aeiou. 2020. Available online: <https://zap.aeiou.pt/tempestades-elsa-fabien-34-milhoes-303912> (accessed on 8 March 2021).
39. Hersbach, H.; Bell, W.; Berrisford, P.; Horányi, A.; Sabater, J.M.; Nicolas, J.; Radu, R.; Schepers, D.; Simmons, A.; Soci, C.; et al. Global reanalysis: Goodbye ERA-Interim, hello ERA5. *ECMWF Newsl.* **2019**, *159*, 17–24. [CrossRef]
40. Cornes, R.C.; Van Der Schrier, G.; Besselaar, E.V.D.; Jones, P.D. An Ensemble Version of the E-OBS Temperature and Precipitation Data Sets. *J. Geophys. Res. Atmos.* **2018**, *123*, 9391–9409. [CrossRef]
41. Tabari, H.; Willems, P. Lagged influence of Atlantic and Pacific climate patterns on European extreme precipitation. *Sci. Rep.* **2018**, *8*, 1–10. [CrossRef] [PubMed]
42. Manning, C.; Widmann, M.; Bevacqua, E.; Van Loon, A.F.; Maraun, D.; Vrac, M. Increased probability of compound long-duration dry and hot events in Europe during summer (1950–2013). *Environ. Res. Lett.* **2019**, *14*, 094006. [CrossRef]
43. Hofstra, N.; Haylock, M.; New, M.; Jones, P.D. Testing E-OBS European high-resolution gridded data set of daily precipitation and surface temperature. *J. Geophys. Res. Space Phys.* **2009**, *114*, 21101. [CrossRef]
44. Herrera, S.; Cardoso, R.M.; Soares, P.M.; Espírito-Santo, F.; Viterbo, P.; Gutiérrez, J.M. Iberia01: A new gridded dataset of daily precipitation and temperatures over Iberia. *Earth Syst. Sci. Data* **2019**, *11*, 1947–1956. [CrossRef]
45. Hersbach, H.; Bell, B.; Berrisford, P.; Biavati, G.; Horányi, A.; Muñoz Sabater, J.; Nicolas, J.; Peubey, C.; Radu, R.; Rozum, I.; et al. ERA5 Hourly Data on Single Levels from 1979 to Present. Copernicus Climate Change Service (C3S) Climate Data Store (CDS). 2018. Available online: [10.24381/cds.adbb2d47](https://cds.adbb2d47). (accessed on 20 April 2021).
46. McKee, T.B.; Doesken, N.J.; Kleist, J. The relationship of drought frequency and duration to time scales. In Proceedings of the 8th Conference on Applied Climatology, Boston, MA, USA, 17–22 January 1993; Volume 17, pp. 179–183.
47. Kalkstein, L.S.; Tan, G.; Skindlov, J.A. An Evaluation of Three Clustering Procedures for Use in Synoptic Climatological Classification. *J. Clim. Appl. Meteorol.* **1987**, *26*, 717–730. [CrossRef]
48. Wilks, D.S. *Statistical Methods in the Atmospheric Sciences*; Elsevier: Amsterdam, The Netherlands, 2011.
49. Bednorz, E.; Wrzesiński, D.; Tomczyk, A.M.; Jasik, D. Classification of Synoptic Conditions of Summer Floods in Polish Sudeten Mountains. *Water* **2019**, *11*, 1450. [CrossRef]
50. Unal, Y.; Kindap, T.; Karaca, M. Redefining the climate zones of Turkey using cluster analysis. *Int. J. Clim.* **2003**, *23*, 1045–1055. [CrossRef]
51. Zolfaghari, F.; Khosravi, H.; Shahriyari, A.; Jabbari, M.; Abolhasani, A. Hierarchical cluster analysis to identify the homogeneous desertification management units. *PLoS ONE* **2019**, *14*, e0226355. [CrossRef]
52. Ferreira, L.; Hitchcock, D.B. A Comparison of Hierarchical Methods for Clustering Functional Data. *Commun. Stat. Simul. Comput.* **2009**, *38*, 1925–1949. [CrossRef]
53. Vicente-Serrano, S.M.; Beguería, S.; López-Moreno, J.I. A Multiscalar Drought Index Sensitive to Global Warming: The Standardized Precipitation Evapotranspiration Index. *J. Clim.* **2010**, *23*, 1696–1718. [CrossRef]
54. Stojanovic, M.; Drumond, A.; Nieto, R.; Gimeno, L. Anomalies in Moisture Supply during the 2003 Drought Event in Europe: A Lagrangian Analysis. *Water* **2018**, *10*, 467. [CrossRef]
55. Vicente-Serrano, S.M.; Aguilar, E.; Martínez, R.; Martín-Hernández, N.; Azorin-Molina, C.; Sanchez-Lorenzo, A.; El Kenawy, A.; Tomás-Burguera, M.; Moran-Tejeda, E.; López-Moreno, J.I.; et al. The complex influence of ENSO on droughts in Ecuador. *Clim. Dyn.* **2017**, *48*, 405–427. [CrossRef]
56. Drumond, A.; Stojanovic, M.; Nieto, R.; Vicente-Serrano, S.M.; Gimeno, L. Linking Anomalous Moisture Transport And Drought Episodes in the IPCC Reference Regions. *Bull. Am. Meteorol. Soc.* **2019**, *100*, 1481–1498. [CrossRef]
57. Salah, Z.; Nieto, R.; Drumond, A.; Gimeno, L.; Vicente-Serrano, S.M. A Lagrangian analysis of the moisture budget over the Fertile Crescent during two intense drought episodes. *J. Hydrol.* **2018**, *560*, 382–395. [CrossRef]

58. Sordo-Ward, A.; Bejarano, M.D.; Iglesias, A.; Asenjo, V.; Garrote, L. Analysis of Current and Future SPEI Droughts in the La Plata Basin Based on Results from the Regional Eta Climate Model. *Water* **2017**, *9*, 857. [CrossRef]
59. Wang, R.; Peng, W.; Liu, X.; Wu, W.; Chen, X.; Zhang, S. Responses of Water Level in China's Largest Freshwater Lake to the Meteorological Drought Index (SPEI) in the Past Five Decades. *Water* **2018**, *10*, 137. [CrossRef]
60. Heim, R.R. A Review of Twentieth-Century Drought Indices Used in the United States. *Bull. Am. Meteorol. Soc.* **2002**, *83*, 1149–1166. [CrossRef]
61. Svoboda, M.; LeComte, D.; Hayes, M.; Heim, R.; Gleason, K.; Angel, J.; Rippey, B.; Tinker, R.; Palecki, M.; Stooksbury, D.; et al. The Drought Monitor. *Bull. Am. Meteorol. Soc.* **2002**, *83*, 1181–1190. [CrossRef]
62. McRoberts, D.B.; Nielsen-Gammon, J.W. The Use of a High-Resolution Standardized Precipitation Index for Drought Monitoring and Assessment. *J. Appl. Meteorol. Clim.* **2012**, *51*, 68–83. [CrossRef]
63. Espinosa, L.A.; Portela, M.M.; Rodrigues, R. Spatio-temporal variability of droughts over past 80 years in Madeira Island. *J. Hydrol. Reg. Stud.* **2019**, *25*, 100623. [CrossRef]
64. Beguería, S.; Vicente-Serrano, S.M.; Gracia, F.R.; Latorre, B. Standardized precipitation evapotranspiration index (SPEI) revisited: Parameter fitting, evapotranspiration models, tools, datasets and drought monitoring. *Int. J. Clim.* **2014**, *34*, 3001–3023. [CrossRef]
65. World Meteorological Organization. *Standardized Precipitation Index User Guide*; World Meteorological Organization: Geneva, Switzerland, 2012; WMO-No. 1090; ISBN 978-92-63-11091-6.
66. Hargreaves, G.H.; Samani, Z.A. Reference Crop Evapotranspiration from Temperature. *Appl. Eng. Agric.* **1985**, *1*, 96–99. [CrossRef]
67. Trigo, R.M.; Dacamara, C.C. Circulation weather types and their influence on the precipitation regime in Portugal. *Int. J. Clim.* **2000**, *20*, 1559–1581. [CrossRef]
68. Martins, D.; Raziei, T.; Paulo, A.A.; Pereira, L.S. Spatial and temporal variability of precipitation and drought in Portugal. *Nat. Hazards Earth Syst. Sci.* **2012**, *12*, 1493–1501. [CrossRef]
69. Miranda, P.; Coelho, F.E.; Tomé, A.R.; Valente, M.A.; Carvalho, A.; Pires, C.; Pires, H.O.; Pires, V.C.; Ramalho, C. 20th century Portuguese Climate and Climate Scenarios. In *Climate Change in Portugal: Scenarios, Impacts and Adaptation Measures (SIAM Project)*; Santos, F.D., Forbes, K., Moita, R., Eds.; Gradiva: New York, NY, USA, 2002; Volume 23–83, p. 454.
70. Ferreira, J.A.; Liberato, M.L.; Ramos, A. On the relationship between atmospheric water vapour transport and extra-tropical cyclones development. *Phys. Chem. Earth Parts A/B/C* **2016**, *94*, 56–65. [CrossRef]
71. Meteovigo. 2019. Available online: <http://www.meteovigo.es/observacion/articulos/item/1149-analisis-de-la-evolucion-atmosferica-ciclon-fabien-21-12-19.html> (accessed on 21 April 2021).
72. Dos Santos, J.C.A.; Corte-Real, J.A.M.; Leite, S. Weather regimes and their connection to the winter rainfall in Portugal. *Int. J. Clim.* **2005**, *25*, 33–50. [CrossRef]
73. RR.sapo. 2019. Available online: <https://rr.sapo.pt/2019/12/20/pais/mau-tempo-continua-depois-da-elsa-vem-ai-a-tempestade-fabien/noticia/175912/> (accessed on 8 March 2021).
74. Pais. 2019. Available online: <https://www.dn.pt/pais/a-dimensao-das-cheias-no-mondego-vista-por-satelite-11649697.html> (accessed on 24 May 2021).
75. EDP. 2019. Available online: <https://www.edpdistribuicao.pt/sites/edd/files/2020-07/Relat%C3%B3rio%20da%20Qualidade%20de%20Servi%C3%A7o%202019%20vf.pdf>. (accessed on 8 March 2021).
76. Copernicus Emergency Management Service ((© 2021 European Union), [EMSR417] Coimbra: Delineation Map, Monitoring 3. Available online: https://emergency.copernicus.eu/mapping/ems-product-component/EMSR417_AOI01_DEL_PRODUCT_r1_RTP01/1?fbclid=IwAR18k8aahqdq7ehK0sUAX5ntPTTrVbkE8O7QG-gXQdxmPx4CwnIM2VbNIBz8 (accessed on 8 March 2021).